Purification and Characterization of the HndA Subunit of NADP-Reducing Hydrogenase from *Desulfovibrio fructosovorans* Overproduced in *Escherichia coli*†

Gilles De Luca,*,‡,§ Marcel Asso,‡ Jean-Pierre Bélaïch,‡,§ and Zorah Dermoun‡,§

Laboratoire de Bioénergétique et Ingéniérie des Protéines, Centre National de la Recherche Scientifique, IFR C1, 31 Chemin Joseph Aiguier, 13402 Marseille Cedex 20, France, and Université de Provence, 3 place Victor Hugo, 13331 Marseille Cedex 3, France

Received October 7, 1997; Revised Manuscript Received December 1, 1997

ABSTRACT: Based on the DNA sequence of its structural genes, clustered in the *hnd* operon, the NADP-reducing hydrogenase of *Desulfovibrio fructosovorans* is thought to be a heterotetrameric complex in which HndA and HndC constitute the NADP-reducing unit and HndD constitutes the hydrogenase unit, respectively. The weak representativity of the enzyme among cell proteins has prevented its purification. This paper discusses the purification and characterization of the HndA subunit of this unique tetrameric iron hydrogenase overproduced in *Escherichia coli*. The purified subunit contains 1.7 mol of non-heme iron and 1.7 mol of acid-labile sulfide/mol. EPR analysis of the reduced form of HndA indicates that it contains a single binuclear [2Fe-2S] cluster. This cluster exhibits a spectrum of rhombic symmetry with values of g_x, g_y, and g_z equal to 1.915, 1.950, and 2.000, respectively, and a midpoint redox potential of −395 mV. The UV−visible and EPR spectra of the [2Fe-2S] cluster indicate that HndA belongs to the [2Fe-2S] family typified by the *Clostridium pasteurianum* [2Fe-2S] ferredoxin. The C-terminal sequence of HndA shows 27% identity with the C-terminal sequence of the 25-kDa subunit of NADH: quinone oxidoreductase from *Paracoccus denitrificans*, 33% identity with the C-terminal sequence of the 24-kDa subunit from *Bos taurus* complex I, and 32% identity with the entire sequence of *C. pasteurianum* [2Fe-2S] ferredoxin. The four cysteine residues involved in HndA cluster binding have been tentatively identified on the basis of sequence identity considerations. Evidence of a HndA organization based on two independent structural domains is discussed.

Hydrogenases (hyds) are iron−sulfur enzymes that catalyze the reversible oxidation of H_2 (*1*). A comparison of their properties reveals that they are a fairly heterogeneous enzyme group that differ in molecular composition, specific activity in catalyzing H_2 oxidation and H_2 production, electron carrier specificity, cofactor content, and sensitivity to inactivation by oxygen (*2*). Three classes of hydrogenases, defined on the basis of their active site metal contents, have been found in *Desulfovibrio* species: nickel hydrogenase ([NiFe] hyds), nickel selenium hydrogenase ([NiFeSe] hyds), and iron-only hydrogenase ([Fe] hyds) (*3*). All these hyds are generally dimeric in *Desulfovibrio* species as confirmed by the analysis of their structural genes (*4*, *5*). The *Desulfovibrio fructosovorans* strain differs from all other *Desulfovibrio* species by its ability to degrade fructose (*6*, *7*). This organism possesses a well-characterized periplasmic [NiFe] hydrogenase (*8*) encoded by the *hynABC* operon and a classical dimeric periplasmic [Fe] hydrogenase which has recently been partially purified (Casalot et al., personal communication). In addition, a NADP-reducing hydrogenase, encoded by an operon made up of four genes named *hndA*, *hndB*, *hndC*, and *hndD*, has been detected in *D. fructosovorans* (*9*). *hndA* and *hndC* encode the NADP-reducing unit, and *hndD* encodes the [Fe] hydrogenase unit; the role of the *hndB* product remains unknown. This cytoplasmic heterotetrameric enzyme, which may bind a great number of iron−sulfur clusters and FMN cofactors, can effect H_2-driven NADP reductions (*9*). The discovery of this NADP-reducing hydrogenase led us to consider the existence of a fourth type of hydrogenase found in *Desulfovibrio* species. Mutagenesis conducted to elucidate the role of the NADP-reducing hydrogenase in *D. fructosovorans* showed that this protein may contribute to energy supply (*8*) despite the low enzyme levels present in the cells. This weak representativity among cell proteins (0.04% of soluble proteins) has, so far, prevented its purification (De Luca et al., unpublished experiments). It was thus decided to attempt to purify and characterize this unique tetrameric iron hydrogenase by inducing overexpression of each subunit encoding gene. It is hoped that this approach will provide sufficient amounts of the subunit to perform reconstitution of the whole complex, including biochemical and structural studies. The characterization of the HndA subunit is the first step of this study. A previous study (*9*) has shown that the HndA subunit displays 29, 21, and 26% identity with the 24

† This work was supported by grants from the Centre de la Recherche Scientifique, the Université de Provence, and the Région Provence-Alpes-Côte d'azur.

* Author to whom correspondence should be addressed at Laboratoire de Bioénergétique et Ingéniérie des Protéines, CNRS, 31 Chemin Joseph Aiguier, 13402 Marseille Cedex 20, France. Telephone: (33) (0) 4 91 16 41 43. Fax: (33) (0) 4 91 71 33 21. E-mail: deluca@ibsm.cnrs-mrs.fr.

‡ Laboratoire de Bioénergétique et Ingéniérie des Protéines, CNRS.

§ Université de Provence.

S0006-2960(97)02474-4 CCC: $15.00 © 1998 American Chemical Society
Published on Web 02/05/1998

kDa subunit from the *Bos taurus* complex I (*10*), the 25 kDa subunit of the NADH:quinone oxidoreductase from *Paracoccus denitrificans* (*11*), and the N-terminal domain of the HoxF subunit (α subunit) of NAD-reducing hydrogenase from *Alcaligenes eutrophus* (*12*), respectively. The 24- and 25-kDa subunits of mammalian and bacterial proteins were characterized (*13, 14*), respectively. They contain a single [2Fe-2S][1] cluster bound by four conserved cysteine ligands (*13, 15*). Such a cluster is thought to be present in HndA. This paper describes the expression of the *hndA* encoding gene in *Escherichia coli* using the pET22(+) vector and the characterization of the HndA subunit of *D. fructosovorans* NADP-reducing hydrogenase.

MATERIALS AND METHODS

Strain and Plasmid. Escherichia coli BL21 (DE3) [F^- *ompT hsdS* (r^-_B m^-_B) *gal dcm* (DE3)] (Novagen) was used as a host for the recombinant plasmid.

An oligonucleotide primer was designated to generate a *Nde*I recognition site at the *hndA* initiation codon: GTTTTCATATGCAAAAACTCAACTTGC. The second oligonucleotide primer was chosen at the end of *hndC*, including a *Bam*HI recognition site. The 2.5 kb fragment obtained after PCR amplification was inserted in the pET22 b(+) vector (Novagen) to obtain a pET-hndABC plasmid. This recombinant plasmid was used to transform *E. coli* BL21 (DE3) for heterologous expression experiments.

Heterologous Production of the HndA Subunit. Competent *E. coli* BL21 (DE3) were transformed with pET-hndABC. pET-hndABC transformed cells lifted from LB agar plates containing 100 μg/mL ampicillin were grown at 37 °C in 30 mL of LB including ampicillin (100 μg/mL) to the late exponential growth phase. This suspension was mixed at a 1:1 ratio with 60% glycerol and frozen at −70 °C. This suspension (200 μL) was partially thawed on ice and inoculated in 6 × 500 mL of LB medium including 100 μg/mL ampicillin and 10 mL of 60% glycerol. Ferric ammonium citrate (10 μg/mL) and sodium sulfide (10 μM) were added to the medium. Cells were grown at 37 °C to $OD_{600\ nm}$ = 2.0 and then stored at 4 °C on ice for half an hour. IPTG was subsequently added (final concentration of 0.5 mM), and the cells were grown for 15 h at 15.3 °C. The cells were harvested by centrifugation at 5000*g* for 10 min.

Purification of the HndA Subunit. The cells were harvested and resuspended in 25 mM Tris-HCl (pH 8.0) (hereafter designated TB), 1 mM EDTA, and 0.1 mM PMSF buffer containing DNase I. The cells were broken up in a French press and subsequently centrifuged twice at 20000*g* for 10 min. Potassium acetate was added to the supernatant to a final concentration of 1 M and then loaded on a phenyl Sepharose CL-6B fast flow (Pharmacia) equilibrated with the same buffer. The HndA-containing fractions were eluted with 40% ethylene glycol, pooled, and then directly loaded on a Q Sepharose fast flow (Pharmacia) equilibrated with TB. Elution was performed using a linear gradient of 0 to 300 mM NaCl. The colored fractions were pooled and loaded on a Hydroxyapatite HTP-Biogel (Bio-rad) equilibrated with TB. Elution with a linear gradient of 0 to 100 mM Na_2HPO_4−NaOH (pH 8.0) allowed us to obtain the purified HndA subunit on the basis of SDS−PAGE analysis and N-terminal partial sequence. The purified HndA was immediately subjected to various assays.

Spectrophotometric Redox Titration and EPR Spectroscopy. The spectrophotometric redox titrations were monitored by performing absorbance measurements at 460 nm with a Kontron Uvikon 932 spectrophotometer on a 40 μM HndA solution in 0.025 M Tris-HCl (pH 8.0) kept under an argon atmosphere. The potentials were checked at 24 °C with a combined micro platinum Metrohm electrode and adjusted with small amounts of a concentrated solution of dithionite (20 mM) in the presence of benzyl viologen (−350 mV) and methyl viologen (−440 mV) at concentration of 2 μM each. EPR spectra were recorded on a Brucker ESP 300-E spectrophotometer equipped with an Oxford instrument ESR-900 helium flow cryostat and a ITC4 temperature controller.

Electrochemical Redox Titration. A three-electrode system consisting of a Metrohm Ag/AgCl (saturated NaCl) reference electrode, a platinum wire auxiliary electrode, and a permselective-membrane pyrolytic graphite working electrode was used for electrochemical titration. An EG&G 273 potentiostat controlled by a Prolinea 4/66 microcomputer with EG&G PARC 270/250 software was used for square-wave voltammetry (SWV). Square-wave voltammograms were obtained with 40 μM HndA (2 μL sample) in 0.025 M Tris-HCl (pH 8) kept under an argon atmosphere at 24 °C, using the following parameters: square-wave frequency, 5 Hz; scan increment, 2 mV; and pulse height amplitude, 25 mV.

Isoelectric Point Measurement. Isoelectric point was determined by performing isoelectric focusing using a Phast gel apparatus from Pharmacia LKB Biotechnology. Phast Gel IEF 3−9, which operates in the 3−9 pH range, was used with a Pharmacia broad-range p*I* calibration kit containing proteins with various isoelectric points ranging from 3 to 10.

Others Analytical Procedures. SDS−polyacrylamide gel electrophoresis was carried out by the method of Laemmli (*16*), with a precast 4 to 20% polyacrylamide (Novex) gel. Low Molecular Weight Markers were from Pharmacia. Protein concentration was routinely estimated by the method of Lowry et al. (*17*) and also by quantitative amino acid analysis for pure protein preparations. Amino acid analysis was performed on a Waters Pico-tag amino acid analysis system. Amino terminal sequence analysis was performed by stepwise Edman degradation using a gas-phase sequencer (Models 470 A, Applied Biosystems). The iron content of the protein was estimated by plasma emission spectroscopy using a Jobin-Yvon model JY 38 apparatus. Acid-labile sulfide was determined according to Forgo and Popowski (*18*) as modified by Lovenberg et al. (*19*).

RESULTS

Production and Purification of the HndA Subunit of D. fructosovorans NADP-Reducing Hydrogenase in E. coli. The

[1] Abbreviations: EPR, electron paramagnetic resonance; [2Fe-2S], binuclear iron−sulfur cluster; Complex I, mitochondrial energy-transducing NADH:quinone oxidoreductase(s); IPTG, isopropyl β-D-thiogalactopyranoside; PMSF, phenylmethanesulfonyl fluoride; DNase I, deoxyribonuclease I; SDS−PAGE, sodium dodecyl sulfate−polyacrylamide gel electrophoresis; kDa, kilodaltons; IEF, isoelectrofocusing; *Pd*, *Paracoccus denitrificans*; *Cp*, *Clostridium pasteurianum*; *Bt*, *Bos taurus*; mT, millitesla; GHz, gigahertz; 2D-NMR, two-dimensional nuclear magnetic resonance.

induction of an *E. coli* strain hosting pET-hndABC for 3 h at 37 °C led to a strong expression of HndA, a weak expression of HndB and an even weaker production of HndC. The proteins were localized in inclusion bodies. Attempts were thus made to determine the optimum induction conditions in 50 mL of LB which led to the production of a folded HndA subunit. The temperature at which the induction was performed was decreased in order to slow growth and thus provide enough time for cofactor incorporation and proper folding of the expressed product. At 25 °C, HndA was still localized in inclusion bodies. Cells were induced overnight at 15 °C using 0.5 mM IPTG. EPR spectrum analysis was performed on this concentrated soluble fraction. After reduction with dithionite, a very weak EPR spectrum of rhombic symmetry was detected, reflecting the presence of a [2Fe-2S] cluster in the soluble extracts (data not shown). The absence of a signal in noninduced *E. coli* pET-hndABC indicates the presence of a functional HndA subunit in *E. coli* pET-hndABC induced at 15 °C. As a result, larger scale purifications were attempted.

The pellet of 3 L of induced *E. coli* pET-hndABC cells showed a brownish-red color which was the reflection of the overproduction of HndA with correct integration of iron−sulfur cluster in these cells. Cells were broken once in a French press, and subsequently centrifuged twice at 20000*g* for 10 min. The crude extract was then centrifuged at 200000*g* for 1 h to obtain a soluble extract. At this stage, the protein was partly found in the pellet, as indicated by its brownish-red color. An additional overnight centrifugation at the same speed, however, resulted in HndA-free supernatant. It would therefore appear that HndA tends to aggregate and precipitate in the absence of its three partners. To avoid sedimentation of HndA and thus increase the yield of purification, crude extracts were directly loaded on phenyl Sepharose. As expected, HndA proved to be very hydrophobic and 40% ethylene glycol was needed to elute the protein from phenyl Sepharose. At this time, the UV−visible spectrum exhibited a pattern attributable to a red-colored protein which was mostly due to the presence of the HndA subunit in this fraction. In Figure 1, the SDS−PAGE patterns of lysate of *E. coli* [pET-hndABC] cells are presented as are the purification steps for the HndA subunit. Approximately 6 mg of purified protein was obtained from 17 g (wet weight) of *E. coli* cells. Purity of the HndA subunit was checked by SDS−PAGE and N-terminal partial sequence of the red hydroxyapatite fractions. The determined sequence, MQN(S)T(C)Q, matches the amino acid sequence deduced from the HndA encoding gene (*9*). HndA subunit molecular mass was estimated to be 19 kDa from SDS−PAGE. The amino acid composition of the purified HndA subunit is consistent with that calculated from the primary structure. IEF−PAGE gel indicated a p*I* of approximately 4.7 for the HndA subunit.

Iron−Sulfur Cluster. Previous analysis of the HndA primary structure suggested the presence of a putative iron−sulfur binding site (*9*). The presence of non-heme iron and acid-labile sulfide was therefore analyzed in the recombinant *D. fructosovorans* HndA subunit. Cells were grown in the presence of ferric ammonium citrate (10 μg/mL) and sodium sulfide (10 μM) as previously described for the 25-kDa subunit of the NADH:quinone oxidoreductase of *Paracoccus denitrificans* (hereafter designated *Pd* 25K) (*14*). The

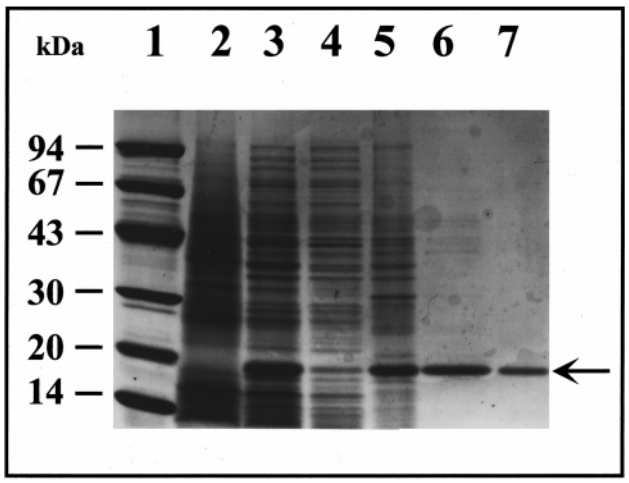

FIGURE 1: Purification steps of the HndA subunit from *E. coli* shown by SDS−PAGE: (1) Low Molecular Weight Markers (Pharmacia), (2) lysate of noninduced *E. coli* [pET-hndABC] cells (200 μg), (3) lysate of induced *E. coli* [pET-hndABC] cells (200 μg), (4) crude extract (20 μg), (5) phenyl Sepharose fraction (10 μg), (6) Q Sepharose fraction (5 μg), (7) purified HndA subunit after hydroxyapatite (1 μg). The arrow indicates the position of the HndA subunit (≈19 kDa).

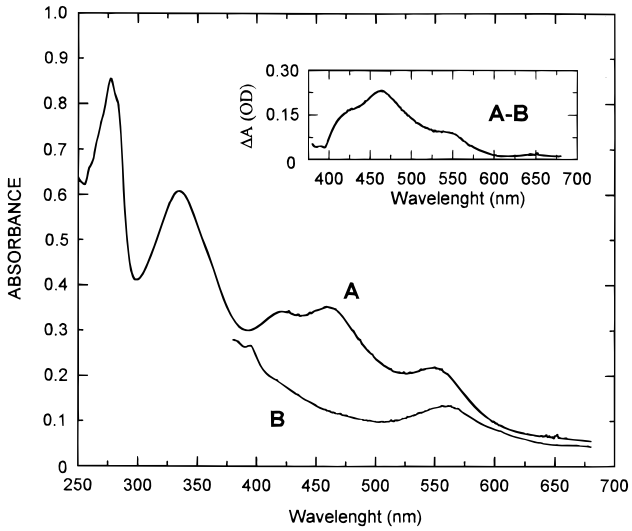

FIGURE 2: Absorption spectra of the purified HndA subunit. Curve A, UV−visible absorption spectrum of the oxidized form of the HndA subunit (40 μM) in 25 mM Tris-HCl (pH 8.0) under argon; curve B, absorption spectrum of the reduced form of the HndA subunit after stepwise addition of sodium dithionite under argon. Curve in the inset (A−B), spectrum difference between oxidized and reduced forms.

purified subunit contains 1.7 mol of non-heme iron and 1.7 mol of acid-labile sulfide/mol of subunit when using the protein concentration determined by amino acid analysis which is likely to be more accurate than the colorimetric dosage (*20*). These results suggest that the HndA subunit carries an iron sulfur cluster as has been previously expected (*9*).

The optical absorption spectrum of the *D. fructosovorans* HndA subunit exhibits four broad peaks at approximately 334, 420, 460, and 550 nm (Figure 2, curve A). This absorption spectrum appears to be very similar to that of *Clostridium pasteurianum* [2Fe-2S] ferredoxin (hereafter designated *Cp* 2Fe Fd) (*21*) and *Pd* 25K (*14*). Addition of sodium dithionite significantly quenched the absorption of

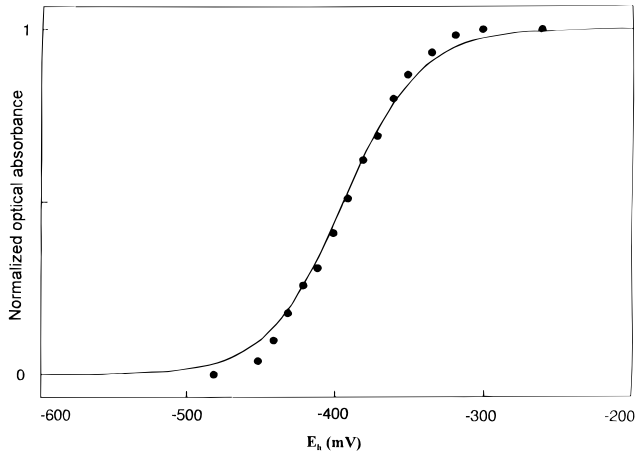

FIGURE 3: Reductive titration of the HndA subunit with dithionite monitored by optical absorbance measurements at 460 nm. The normalized variations correspond to the ratio $[A_{460(ox)} - A_{460(E)}]/[A_{460(ox)} - A_{460(red)}]$. The solid line is the best fit of the data with a Nernst curve centered at −395 mV.

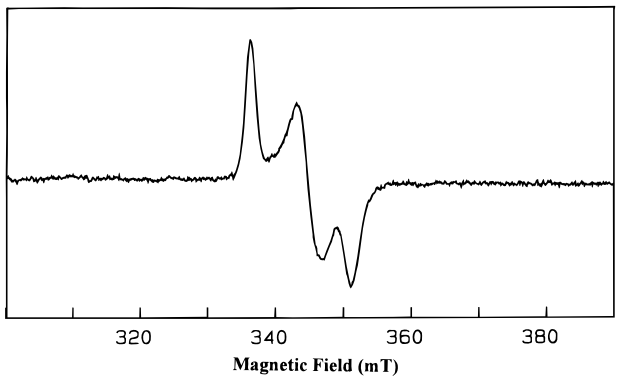

FIGURE 4: EPR spectrum of the HndA subunit. EPR spectrum was performed with 40 μM HndA subunit in 25 mM Tris-HCl (pH 8.0) and reduced with dithionite. EPR spectrum was recorded under the following conditions: microwave frequency, 9.418 GHz; microwave power, 4 mW; modulation amplitude, 1 mT; and sample temperature, 80 K. EPR values are g_x, g_y, and g_z equal to 1.915, 1.950, and 2.000, respectively.

the expressed HndA subunit throughout the entire wavelength range as shown in Figure 2, curve B. The redox behavior of the iron−sulfur center was monitored by studying band variation (460 nm) as a function of solution potential. The experimental data were fitted as a Nernst curve centered at −395 mV (±5 mV) (Figure 3) and are in good agreement with the −400 mV value obtained by electrochemical measurements. The $A_{460\ nm}/A_{280\ nm}$ ratio of pure protein is 0.43. Iron−sulfur content was used to determine that approximately 85% of purified HndA subunits contain an iron−sulfur cluster. Thus, concentration of iron−sulfur cluster-ligated HndA subunits was estimated to represent 85% of total purified HndA. The molar extinction coefficients for the most pronounced features of the Fe−S chromophore were determined to be 5000 M^{-1} cm^{-1} at 550 nm, 8400 M^{-1} cm^{-1} at 460 nm, 8100 M^{-1} cm^{-1} at 420 nm, and 14450 M^{-1} cm^{-1} at 334 nm for oxidized samples and 3350 M^{-1} cm^{-1} at 556 nm for dithionite-reduced samples. These results support the hypothesis that the expressed HndA subunit ligates functional redox iron−sulfur cluster(s).

The EPR spectrum of the purified HndA subunit was examined to determine the iron−sulfur cluster type. After direct reduction of an EPR sample with dithionite, the protein solution exhibited at low temperature a rhombic EPR spectrum characterized by g_x, g_y, and g_z, equal to 1.915, 1.950, and 2.000, respectively (Figure 4). This spectrum was found to be unchanged between 10 and 100 K, and showed relaxation broadening for temperatures higher than 150 K. These spectral characteristics are typical of a $[2Fe\text{-}2S]^+$ cluster, and are very similar to those observed for the *Cp* 2Fe Fd (*22*), for the related *Pd* 25K (*14, 23*), and for the NQO2 subunit from *Thermus thermophilus* HB-8 NADH: quinone oxidoreductase (*24*). The double integration of the spectrum was performed at 80 K. The comparison with a $CuSO_4$ standard showed that it corresponds to about 0.7 spin/molecule, indicating that the major part of the protein molecules coordinates a binuclear cluster. In conclusion, HndA ligates a single binuclear [2Fe-2S] cluster which is in agreement with sequence predictions.

Amino Acid Sequence Similarity with the C. pasteurianum [2Fe-2S] Ferredoxine Family. Spectroscopic properties of the [2Fe-2S] cluster from *Pd* 25K were found to be strikingly similar to the [2Fe-2S] cluster from *Cp* 2Fe Fd (*23*). These two proteins thus constitute a subclass of ferredoxin-type [2Fe-2S] centers (*23*). The assignment of cysteine ligands performed by site-directed mutagenesis (*13, 15, 25*−*27*) revealed the presence of two patterns of cysteine ligands for the binding of the [2Fe-2S] cluster in the *Cp* 2Fe Fd family. *Pd* 25K (*15*) and the 24-kDa subunit from *Bos taurus* Complex I (hereafter designated *Bt* 24K) (*13*) exhibit a $C\text{-}X_4\text{-}C\text{-}X_{35}\text{-}C\text{-}X_3\text{-}C$ pattern, whereas *Cp* 2Fe Fd (*25*−*27*) has a $C\text{-}X_{12}\text{-}C\text{-}X_{31}\text{-}C\text{-}X_3\text{-}C$ pattern. On the basis of the two patterns of cysteine ligands and sequence identities pointed out by the Blast program, the 87−171 C-terminal sequence of HndA has been aligned with the 83−180 C-terminal sequence of *Pd* 25K (*11*), the 87−183 C-terminal sequence of *Bt* 24K (*10*), and the entire sequence of *Cp* 2Fe Fd (*28*) (Figure 5). HndA showed 27% identity and 47% similarity with *Pd* 25K and 33% identity and 52% similarity with *Bt* 24K. The sequence identities were almost uniformly distributed between HndA and *Pd* 25K/*Bt* 24K. In addition, HndA exhibited 32% identity and 40% similarity with *Cp* 2Fe Fd. Two short conserved clusters, P-I-V-(X)-V and Y-G-N-V-T, were identified in the C-terminal region downstream of the C-X-G-X-C pattern. This C-terminal area, which lies between C-139 and Y-171, showed 46% identity and 52% similarity out of 35 residues. The introduction of an eight-residue gap between the two first cysteine ligands in HndA, *Pd* 25K, and *Bt* 24K subunits allowed us to find identity in the N-terminal region. This gap is due to the fact that a poorly structured and possibly solvent-exposed flexible loop can be deleted in *Cp* 2Fe Fd mutants without deleterious effects (*27*). In the N-terminal region, six residues in addition to the first cysteine ligand are conserved (56% identity). The less conserved region lies from M-99 to R-138 in the HndA subunit. This region exhibited 17% identity and 30% similarity with *Cp* 2Fe Fd. In light of this sequence alignment, the conserved C-98, C-103, C-139, and C-143 are the most likely candidates for cluster binding in HndA.

Spontaneous Proteolysis of HndA. Unexpected results were obtained during the desalting preparation for NH_2 terminal sequencing. Indeed, spontaneous proteolysis of the HndA subunit occurred during the desalting preparation performed in a centicron (cutoff, 10 kDa). The HndA

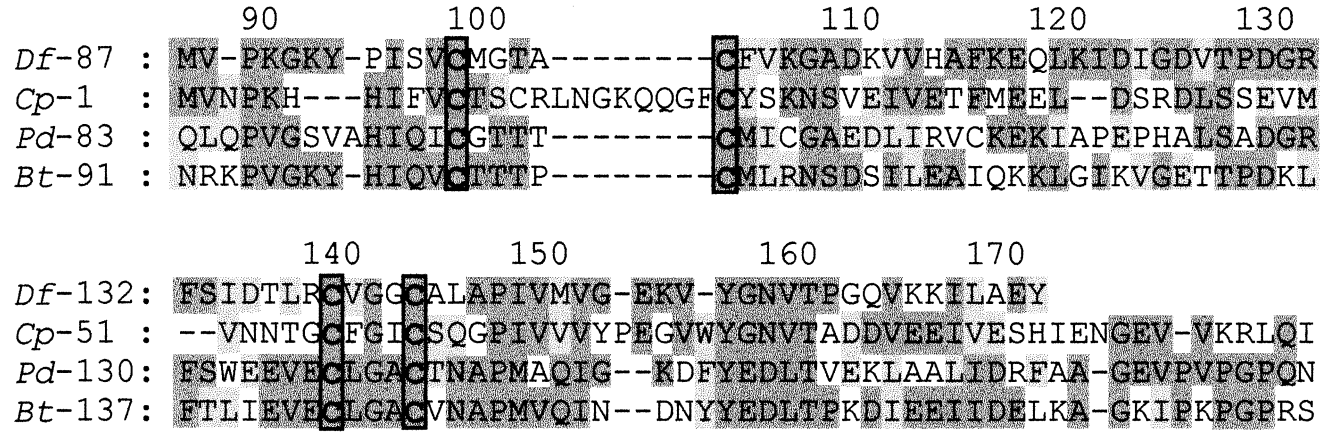

FIGURE 5: Sequence alignement of HndA with the three well-characterized proteins of the [2Fe-2S] family typified by *C. pasteurianum* ferredoxin. *Df*, HndA subunit from *D. fructosovorans* NADP-reducing hydrogenase; *Cp*, [2Fe-2S] ferredoxin from *C. pasteurianum*; *Pd*, 25-kDa subunit from *P. denitrificans* NADH:ubiquinone oxidoreductase (NDH−I); *Bt*, 24-kDa subunit from *B. taurus* Complex I. Identical amino acids are shaded in dark gray; similar amino acids are shaded in pale gray, and cysteine residues present in conserved positions are boxed.

subunit was thus cleaved into three major fragments as revealed by NH_2 terminal sequencing (first sequence, HAV-LPQP; and second sequence, MVPKGKY) and by the presence of two major bands at 17 and 8−9 kDa on SDS−PAGE. A histidine 17-to-tyrosine 171 peptide of 17 kDa, a histidine 17-to-methionine 87 peptide of 7.7 kDa, and a methionine 87-to-tyrosine 171 fragment of 9.2 kDa were generated. The UV−visible spectrum and the redox potential value obtained by electrochemistry of the preparation before and after cleavage appear to be unchanged. The spectrum recorded before cleavage is due to the contribution of the [2Fe-2S] cluster linked to the entire 1−171 HndA subunit. Since the spectrum remains unchanged after proteolysis, it is likely that the 17−171 peptide retains the [2Fe-2S] cluster and that the 87−171 peptide (Figure 5) still ligates the [2Fe-2S] cluster. The very low amounts of the preparation generated did not allow purification and characterization of each peptide.

DISCUSSION

The heterologous expression of the HndA subunit encoding gene of the NADP-reducing hydrogenase from *D. fructosovorans* was successfully achieved in *E. coli*. This recombinant HndA subunit is correctly folded in *E. coli* and contains an air-stable iron−sulfur cluster. Its purification led us to obtain 6 mg of HndA from 17 g (wet weight) of *E. coli* cells. This subunit is an acidic red protein which exhibits hydrophobic properties and tends to aggregate in the absence of its three natural partners. The iron and labile sulfide content, as well as the UV−visible and EPR spectra, revealed that HndA contains a single [2Fe-2S] cluster which is very similar to the [2Fe-2S] center bound in proteins belonging to the *Cp* 2Fe Fd family. The C-terminal region of the HndA subunit presents significant identities with the C-terminal region of two NADH:quinone oxidoreductase subunits homologous to HndA (27/33% identity, 47/52% similarity) and with *Cp* 2Fe Fd (32% identity, 40% similarity). The conserved cysteines C-98, C-103, C-139, and C-143 present a $C\text{-}X_4\text{-}C\text{-}X_{35}\text{-}C\text{-}X_3\text{-}C$ pattern similar to that of *Pd* 25K and are therefore the most likely candidates for cluster binding in HndA. Moreover, HndA subunits exhibit an intermediate redox potential of −395 mV compared to −280 mV for *Cp* 2Fe Fd (*21*) and −456 to −465 mV for the subunits of NADH:quinone oxidoreductase (*14*, *29*). This potential is very close to the −380 mV value of the C16/Δ19−30 molecular variant of *Cp* 2Fe Fd that was constructed to mimic the cysteine ligand pattern of *Pd* 25K in a C14A/C24A mutant (*27*). Deletions occurring in this mutant were found to only marginally modify the spectroscopic properties of the [2Fe-2S] cluster but resulted in variations of its redox potential over a range of nearly 100 mV (−294 to −381 mV). The low degrees of homology (17% identity, 30% similarity) in the HndA region from M-99 to R-138 are in agreement with the hypothesis that the discrepancies between the properties of the *Pd* 25K subunit Fe−S chromophores and *Cp* 2Fe Fd must originate mainly from differences in polypeptide folding in the region of residues 15−30 of *Cp* 2Fe Fd. In light of the sequence alignment, it is not possible to identify the residues directly involved in these modulations of potential between −280 mV and −456 to −465 mV, a range which encompasses −395 mV. Finally, the fact that spontaneous hydrolysis of the HndA subunit results in the production of smaller peptides which still ligate a [2Fe-2S] cluster seems to indicate that the HndA subunit may consist of two structurally independent domains. One ferredoxin-like C-terminal domain may ligate the [2Fe-2S] cluster (Figure 5), and the other could be implicated in the interaction with another/other subunit(s) of the hydrogenase complex. Only 2D-NMR and/or crystallographic studies, soon to be carried out, may provide answers to these questions.

Characterization of the HndA subunit is the first step of an ongoing study. Heterologous overproduction will also be performed for HndB and HndC recombinant subunits in *E. coli* in order to characterize each component of *D. fructosovorans* NADP-reducing hydrogenase. In the case of the HndD recombinant protein, its production will only be attempted in *D. fructosovorans*, since the production of functional iron-only hydrogenase subunit is highly unlikely to occur in *E. coli*. Taken together, these overproductions in heterologous or homologous hosts should enable us to reconstitute the entire hydrogenase complex in vitro and to define the exact role of each partner as well as the relationships existing between them.

ACKNOWLEDGMENT

We thank J. Bonicel for N-terminal sequencing, N. Zylberg for amino acid analysis, J. C. Germanique for the estimation of protein iron content by plasma emission, Dr. P. Bianco for electrochemical titration, and Dr. B. Guigliarelli for EPR measurements and for carefully reading the manuscript. We are grateful to Dr. M. Johnson for correcting the English in the manuscript.

REFERENCES

1. Stephenson, M., and Stickland, L. H. (1931) *Biochem. J. 25*, 205−214.
2. Adams, M. W. W., Mortenson, L. E., and Chen, J. S. (1981) *Biochim. Biophys. Acta 594*, 105−176.
3. Fauque, G., Peck, H. D., Jr., Moura, J. J. G., Huynh, B. H., Berlier, Y., Dervartanian, D. V., Teixeira, M., Przybyla, A. E., Lespinat, P. A., Moura, I., and LeGall, J. (1988) *FEMS Microbiol. Rev. 54*, 299−344.
4. Voordouw, G. E., Brenner, S. (1985) *Eur. J. Biochem. 148*, 515−520.
5. Voordouw, G. E., Menon, N. K., LeGall, J., Peck, H. D., and Przybyla, A. E. (1989) *J. Bacteriol. 171*, 2894−2899.
6. Ollivier, B., Cord-Ruwisch, R., Hatchikian, C. E., and Garcia, J. L. (1988) *Arch. Microbiol. 149*, 447−450.
7. Malki, S., De Luca, G., Fardeau, M. L., Rousset, M., Dermoun, Z., and Bélaïch, J. P. (1997) *Arch. Microbiol. 167*, 38−45.
8. Hatchikian, C. E., Traore, A. S., Fernandez, V. M., and Cammack, R. (1990) *Eur. J. Biochem. 187*, 635−643.
9. Malki, S., Saimmaime, I., De Luca, G., Rousset, M., Dermoun, Z., and Bélaïch, J. P. (1995) *J. Bacteriol. 177*, 2628−2636.
10. Fearnley, I., and Walker, J. E. (1992) *Biochim. Biophys. Acta 1140*, 105−134.
11. Xu, X., Matsuno-Yagi, A., and Yagi, T. (1991) *Biochemistry 30*, 8678−8684.
12. Tran-Betcke, A., Warnecke, U., Bocker, C., Zaborosch, C., and Friedrich, B. (1990) *J. Bacteriol. 172*, 2920−2929.
13. Wilks, P., Walker, J. E., Albracht, S. P. J., and Van Belzen, R. (1995) *Protein Sci. 4* (Suppl. 1), 64.
14. Yano, T., Sled, V. D., Ohnishi, T., and Yagi, T. (1994) *Biochemistry 33*, 494−499.
15. Yano, T., Sled, V. D., Ohnishi, T., and Yagi, T. (1994) *FEBS Lett. 353*, 160−164.
16. Laemmli, U. K. (1970) *Nature 227*, 680−685.
17. Lowry, O. H., Rosebrough, N. J., Farr, A. L., and Randall, R. J. (1951) *J. Biol. Chem. 193*, 265−275.
18. Forgo, J. K., and Popowski, M. (1949) *Anal. Chem. 21*, 732−734.
19. Lovenberg, W., Buchanan, B. B., and Rabinovitz, J. C. (1963) *J. Biol. Chem. 238*, 3899−3913.
20. Adams, M. W. W., Eccleston, E., and Howard, J. B. (1989) *Proc. Natl. Acad. Sci. U.S.A. 86*, 4932−4936.
21. Cardenas, J., Mortenson, L., and Yoch, D. C. (1976) *Biochim. Biophys. Acta 434*, 244−257.
22. Bertrand, P., Gayda, J. P., Fee, J. A., Kuila, D., and Cammack, R. (1987) *Biochim. Biophys. Acta 916*, 24−28.
23. Crouse, B. R., Yano, T., Finnegan, M. G., Yagi, T., and Johnson, M. K. (1994) *J. Biol. Chem. 269*, 21030−21036.
24. Yano, T., Chu, S. S., Sled, V. D., Ohnishi, T., and Yagi, T. (1997) *J. Biol. Chem. 272*, 4201−4211.
25. Fujinaga, J., Gaillard, J., and Meyer, J. (1993) *Biochem. Biophys. Res. Commun. 194*, 104−111.
26. Meyer, J., Fujinaga, J., Gaillard, J., and Lutz, M. (1994) *Biochemistry 33*, 13642−13650.
27. Golinelli, M. P., Akin, L. A., Crouse, B. R., Johnson, M. K., and Meyer, J. (1996) *Biochemistry 35*, 8995−9002.
28. Meyer, J., Bruschi, M. H., Bonicel, J., and Bovier-Lapierre, G. E. (1986) *Biochemistry 25*, 6054−6061.
29. Ohnishi, T., Ragan, C. I., and Hatefi, Y. (1985) *J. Biol. Chem. 260*, 2782−2788.

BI972474P